# Delft University of Technology

Corrigendum to "Crashworthiness in preliminary design
mean crushing force prediction for closed-section thin-walled metallic structures"
[International Journal of Impact Engineering, Volume 188, June 2024,
104946](S0734743X24000708)(10.1016/j.ijimpeng.2024.104946)

Anand, Shreyas; Alderliesten, René; Castro, Saullo G.P.

Corrigendum

# Corrigendum to "Crashworthiness in preliminary design: mean crushing force prediction for closed-section thin-walled metallic structures" [International Journal of Impact Engineering, Volume 188, June 2024, 104946]

Shreyas Anand, René Alderliesten, Saullo G.P. Castro [*]

*TU Delft Faculty of Aerospace Engineering, Kluyverweg 1, Delft, 2629 HS, Zuid Holland, Netherlands*

## ARTICLE INFO

## Abstract

The authors regret to inform that an error has been identified in the numerical dataset presented in the original paper (Appendix C.1) for square tubular structures. The mean force values were taken for the entire range (including the peak) instead of the plateau phase of the crushing due to a scripting error. This has an effect on some of the co-efficient of determination values, error ranges in Table 2 and causes a change in the generalized equation. However, the coefficient of determination of the generalized model remains unchanged. This corrigendum presents the changes in text and the updated figures and tables. The authors would like to apologise for any inconvenience caused.

## Changes in text

### 7.2. Inextensional crushing of square tubular structures

As shown in Fig. 10(a), for square tubular structures the model from Magee and Thornton (Eq. (16)) slightly underpredicts the mean crushing force. Fig. 10(b) presents the comparison based on the model from Abramowicz et al. (Eq. (17)), a good correlation fit is observed between the model and the dataset, with $R^2=0.91$. Finally, the extensional crushing model from Tabacu et al. (Eq. (28)) overpredicts the inexten-sional mean force by a large margin, reaching $R^2=0.50$, the comparison is presented in Fig. 10(c).

## 10. Calibration of Zhang and Zhang's model [15] with our dataset

**In the paragraph after equation 59:** Using this equation from Zhang and Zhang, results in a good fit with experimental/numerical data with an $R^2$ of 0.92. The results using Eq. (59) are presented in Fig. 17.

**After equation 61:** Fig. 18 illustrates the curve fit obtained for our dataset, the equation from Magee and Thornton is also plotted for comparison. From the curve fitting, the parameters $a$ and $b$ were determined to be 52.00 and 0.21 respectively, which indicates a slightly greater sensitivity of the mean crushing force to the edge length for a square tubular structure. Rewriting Eq. (60) based on the obtained values of a and b:

$$\frac{P_m}{M_0} \cdot \kappa = 52 \cdot \left(\frac{c}{h}\right)^{0.21} \tag{62}$$

It is also of interest to use this new expression of Eq. (62) to calibrate the model from Zhang and Zhang (Eq. (57)), aiming to obtain an
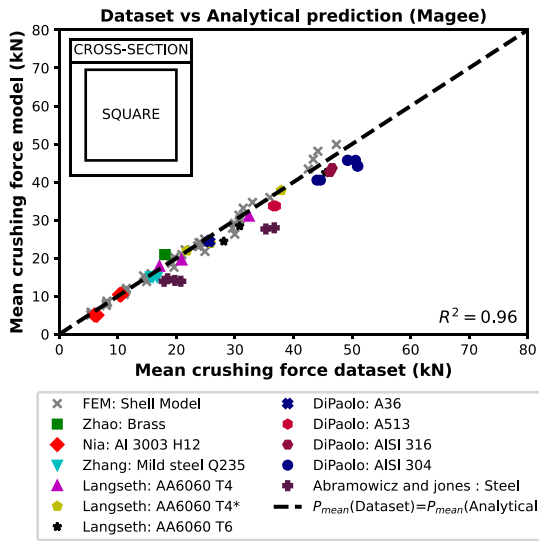
**Fig. 10(a).** Comparison between analytical models and dataset for square tubular structures: (a) Magee and Thornton [25].
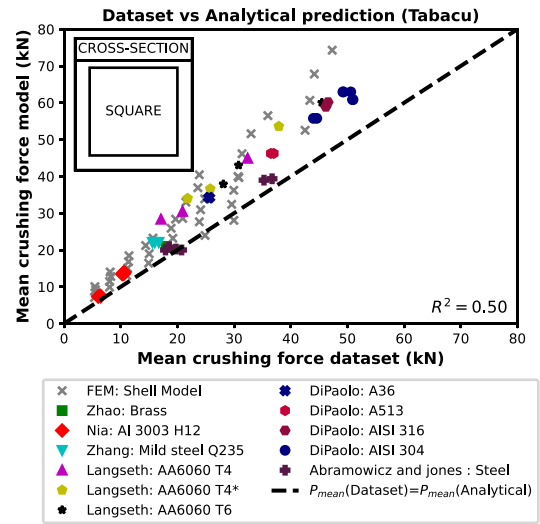


**Fig. 10(c).** Comparison between analytical models and dataset for square tubular structures: (c) Tabacu et al. [2].
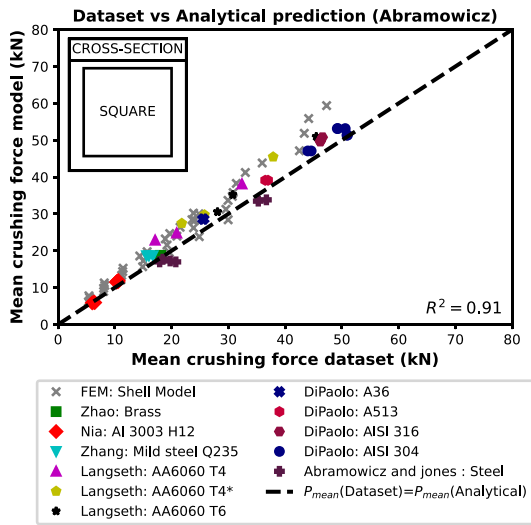


**Fig. 10(b).** Comparison between analytical models and dataset for square tubular structures: (b) Abramowicz et al. [1].
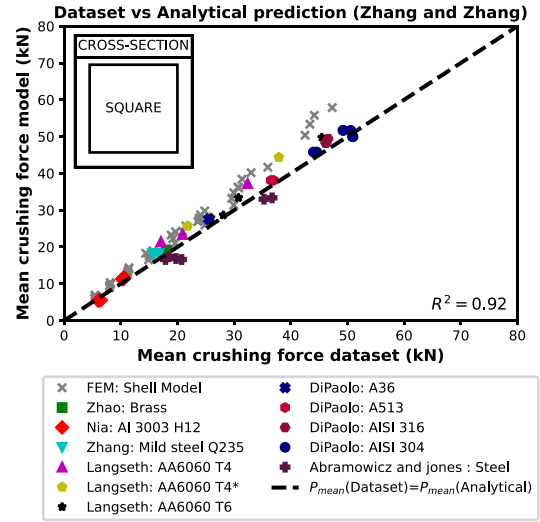


**Fig. 17.** Comparison of the Zhang and Zhang's model [2] for square tubular structures.

expression for inextensional crushing of angle elements. Following the procedure given by Zhang and Zhang [15], the following equation for an angle element is obtained:

$$P_m = \frac{\sigma_0}{2\kappa} \cdot B^{0.21} \cdot h^{1.79} \sqrt{\frac{2\pi \cdot \tan(\theta/2)}{0.105(\tan(\theta/2) + 0.06/\tan(\theta/2))}} \quad (63)$$

Using the material data from [38], a value of 146 MPa for $\sigma_0$ is obtained using Eq. (6). Fig. (19) presents a comparison between the numerical results from Zhang and Zhang (Table 1 in [15]) with the results obtained using Eq. (63). For comparison, the results obtained using Eq. (59) are also plotted, for this equation $\sigma_0 = 106$MPa is retained from the original work. After calibration with our dataset, an even better correlation is observed between the numerical and analytical values, with $R^2$ increasing from 0.987 for calibration using Magee and Thornton's dataset to 0.988 for calibration using our dataset. The $R^2$ value, when only considering elements with $\theta = 90°$, also increases from 0.986 to 0.992 (see Fig. (19)).

Further, this new expression based on Zhang and Zhang's model (Eq. 63) can be used to estimate the mean crushing force for inextensional
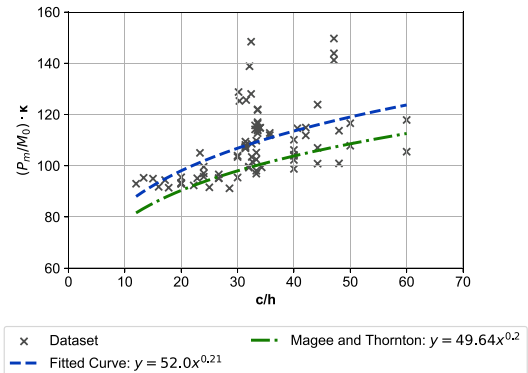


**Fig. 18.** Curve fit for our dataset using Eq. (60).

crushing of hexagonal and octagonal tubular structures (Figs. 20(a) and 20(b)). For hexagonal tubular structures, the $R^2$ value increased from 0.86 to 0.97 and for the octagonal tubular structures, the $R^2$ value
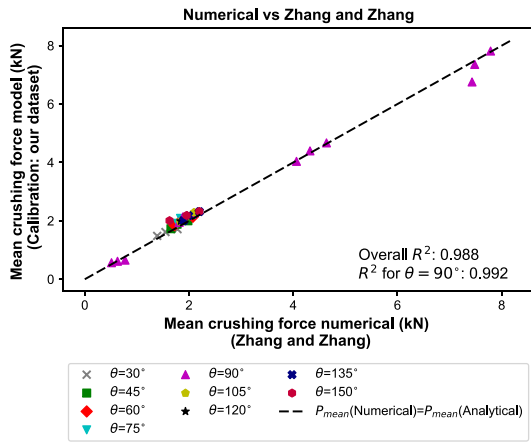
**Fig. 19(a).** Comparison of numerical (FEM results from Zhang and Zhang [15]) and analytical mean crushing force obtained using Zhang and Zhang's model calibrated with (a) Our dataset.
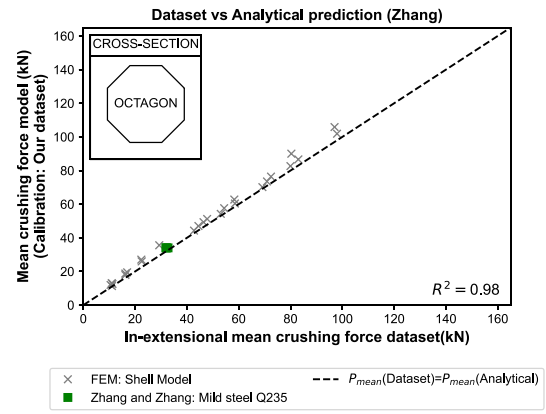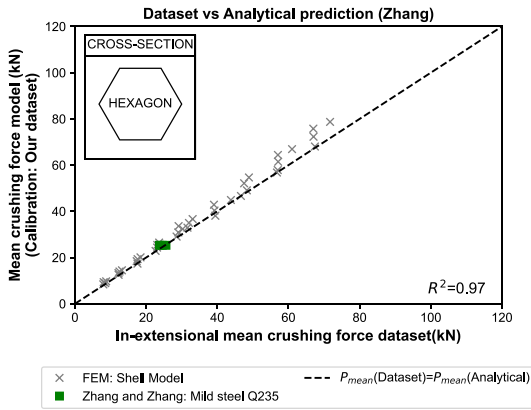


**Fig. 20(a).** Comparison of model from Zhang and Zhang [15] (calibrated with our dataset, Eq. (63)) for (a) hexagonal tubular structures.
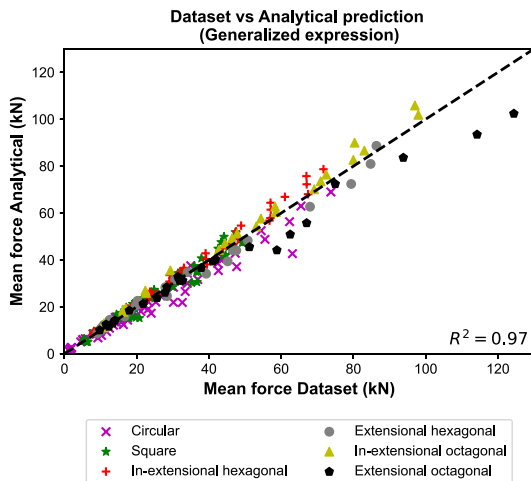


**Fig. 20(b).** Comparison of model from Zhang and Zhang [15] (calibrated with our dataset, Eq. (63)) for (b) octagonal tubular structures.



**Fig. 21.** Comparison between generalized expression for mean crushing force and mean crushing force dataset.

**Table 1**
Values of X, Y and Z for specific cases (Eq. (70)).

| S.No. | Case | X | Y | Z |
|---|---|---|---|---|
| 3 | Polygon (Inext) | 12.57 | 1.03 | 0.21 |

increased from 0.90 to 0.98.

## 11. Generalized mean crushing force expression for axial crushing of metallic tubular structures

$$P_m = \frac{N_c \cdot \sigma_0}{2\kappa} \cdot B^{0.21} h^{1.79} \sqrt{\frac{2\pi \cdot \tan(\theta/2)}{0.105(\tan(\theta/2) + 0.06/\tan(\theta/2))}} \quad (66)$$

$$\frac{P_m}{M_0} \cdot \kappa = 13.37 \left(\frac{c}{h}\right)^{0.21} \sqrt{\frac{N_c^2 \cdot \tan(\theta/2)}{(\tan(\theta/2) + 0.06/\tan(\theta/2))}} \quad (67)$$

$$P_m = 12.57 \cdot N_c^{1.03} \cdot \left(\frac{c}{h}\right)^{0.21} \quad (69)$$

## 12. Discussion

**End of 3rd paragraph reads:** A calibration of Zhang and Zhang's model based on our dataset has also been proposed, which further improves the accuracy of Zhang and Zhang's model for polygonal tubular structures ($R^2$ (hexagonal) = 0.97 and $R^2$ (octagonal) = 0.98).

## 13. Conclusions

**In the 2nd paragraph:** For inextensional crushing of polygonal

**Table 2**
Coefficient of determination (R2), Average error ($\overline{E}$) and Interquartile range for various analytical models.

| Model | Eq. | $R^2$ | $\overline{E}$ (%) | Interquartile range | | |
|---|---|---|---|---|---|---|
| | | | | $Q_1$ | $Q_2$ | $\Delta$ |
| **Square tubular structures** | | | | | | |
| Magee and Thornton | (16) | 0.96 | 4.5 | -1.1 | 7.7 | 8.8 |
| Abramowicz et al. | (17) | 0.91 | -13.0 | -20.8 | -6.1 | 14.8 |
| Tabacu et al. | (30) | 0.50 | -32.9 | -43.9 | -21.3 | 22.6 |
| **Hexagonal tubular structures (Inextensional)** | | | | | | |
| Zhang and Zhang (Our Calibration) | (63) | 0.97 | -6.6 | -9.8 | -2.3 | 7.5 |
| **Octagonal tubular structures (Inextensional)** | | | | | | |
| Zhang and Zhang (Our Calibration) | (63) | 0.98 | -8.52 | -12.1 | -4.0 | 8.1 |

**Table 3**
Numerical dataset for square tubular structures (Appendix C.1).

| S.No. | c (mm) | h (mm) | $P_{mean}$ (kN) Square | |
|---|---|---|---|---|
| | | | AA6060 T4 | AISI 316 |
| 1 | 30 | 1.00 | 5.36 | 20.94 |
| 2 | 30 | 1.25 | 8.03 | 30.70 |
| 3 | 30 | 1.50 | 11.08 | 42.53 |
| 4 | 30 | 1.75 | 14.91 | |
| 5 | 30 | 2.00 | 19.59 | - |
| 6 | 30 | 2.25 | 24.88 | - |
| 7 | 30 | 2.50 | 29.97 | - |
| 8 | 40 | 1.00 | 5.68 | 21.50 |
| 9 | 40 | 1.25 | 8.03 | 31.41 |
| 10 | 40 | 1.50 | 11.21 | 43.38 |
| 11 | 40 | 1.75 | 15.02 | |
| 12 | 40 | 2.00 | 19.20 | - |
| 13 | 40 | 2.25 | 23.87 | - |
| 14 | 40 | 2.50 | 29.58 | - |
| 15 | 50 | 1.00 | 5.56 | 23.61 |
| 16 | 50 | 1.25 | 8.24 | 33.00 |
| 17 | 50 | 1.50 | 11.38 | 44.16 |
| 18 | 50 | 1.75 | 14.40 | |
| 19 | 50 | 2.00 | 18.89 | - |
| 20 | 50 | 2.25 | 24.10 | - |
| 21 | 50 | 2.50 | 29.95 | - |
| 22 | 60 | 1.00 | 5.44 | 23.87 |
| 23 | 60 | 1.25 | 8.13 | 35.97 |
| 24 | 60 | 1.50 | 11.46 | 47.32 |
| 25 | 60 | 1.75 | 15.69 | |
| 26 | 60 | 2.00 | 19.68 | - |
| 27 | 60 | 2.25 | 24.82 | - |
| 28 | 60 | 2.50 | 30.85 | - |

tubular structures, the model from Zhang and Zhang calibrated to our

dataset (Eq. (63)) for square tubular structures gives the best overall accuracy ($R^2$ (hexagonal) = 0.97 and $R^2$ (octagonal) = 0.98).

**Changes in Figures**

Since, a change in the FEM numerical dataset for square tubular structures causes a change in the coefficient of determination values and slight changes in the data-point positions, some figures need to be updated. However, except for Fig. 18, the observed trends remain similar to the original paper. The changed figures are: Figs. 10(a), 10(b), 10(c), 17, 18, 19(a), 20(a), 21 and 20(b).

**Changed entries in tables**

1 entry in Table 1 and 5 entries in Table 2 are changed as a result of the corrections. The changed entries of the table are presented in tables Table 1 and Table 2. The updated values for the square numerical dataset appendix are presented as a new table (Table 3) which replaces a part of Appendix C.1.

**Declaration of competing interest**

The authors declare that they have no known competing financial interests or personal relationships that could have appeared to influence the work reported in this paper.